ASME Journal of Applied Mechanics
Online journal at:
https://asmedigitalcollection.asme.org/appliedmechanics

Ekaterina Antimirova
Department of Mechanical Engineering,
University of California Berkeley,
Berkeley, CA 94720
e-mail: ekatant23@berkeley.edu

Jiyoung Jung
Department of Mechanical Engineering,
University of California Berkeley,
Berkeley, CA 94720
e-mail: jeeyoungek@berkeley.edu

Zilan Zhang
Department of Mechanical Engineering,
University of California Berkeley,
Berkeley, CA 94720
e-mail: shilan@berkeley.edu

Aaron Machuca
Department of Mechanical Engineering,
University of California Berkeley,
Berkeley, CA 94720
e-mail: aaronimachuca@berkeley.edu

Grace X. Gu[1]
Department of Mechanical Engineering,
University of California Berkeley,
Berkeley, CA 94720
e-mail: ggu@berkeley.edu

Overview of Computational Methods to Predict Flutter in Aircraft

Aeroelastic flutter is a dynamically complex phenomenon that has adverse and unstable effects on elastic structures. It is crucial to better predict the phenomenon of flutter within the scope of aircraft structures to improve the design of their wings. This review aims to establish fundamental guidelines for flutter analysis across subsonic, transonic, supersonic, and hypersonic flow regimes, providing a thorough overview of established analytical, numerical, and reduced-order models as applicable to each flow regime. The review will shed light on the limitations and missing components within the previous literature on these flow regimes by highlighting the challenges involved in simulating flutter. In addition, popular methods that employ the aforementioned analyses for optimizing wing structures under the effects of flutter—a subject currently garnering significant research attention—are also discussed. Our discussion offers new perspectives that encourage collaborative effort in the area of computational methods for flutter prediction and optimization. [DOI: 10.1115/1.4064324]

Keywords: aeroelasticity, flutter, stability analysis, computational mechanics, aerodynamics, aircraft design

1 Introduction

Flutter refers to the dynamic instability of an elastic structure exposed to fluid flow past a critical speed threshold. Beyond this threshold, a self-excited feedback loop occurs between body deflection and fluid forces, leading to fatigue in the body and ultimately resulting in structural failure. This dynamic interaction can be represented through a triangle diagram of aeroelastic forces, illustrating the intricate interplay between aerodynamic, elastic, and inertial forces within a body [1]. Any of these three forces can induce instability within the structure. The flutter phenomenon consequently poses serious risk to flexible structures under the influence of fluid forces, particularly aircraft wings subject to aerodynamic forces.

In the case of aeroelastic flutter, during high flight-speed regimes, the aircraft progressively approaches a critical flutter threshold where structural damping mechanisms fail to suppress the amplifying vibrations driven by aerodynamic body loads. Classifications of the accompanying flutter phenomena can be grouped into classical and nonclassical categories [1]. Classical flutter refers to simple harmonic oscillations of a body at a critical speed and its corresponding structural coupling modes. Nonclassical flutter includes additional flow complexities such as flow separation, stall, phase lag, and other nonlinear phenomena. To avoid confusion, it is important to distinguish between the varying definitions of the concept of limit cycle oscillations (LCO) under different flutter classifications. In this article, LCO is referred to as a complex postflutter phenomenon, where considerable structural deflections due to nonlinear effects are otherwise not captured or predicted in classical flutter theory. The critical flutter speed is then referred to as a harmonic oscillation to denote the discrepancies in definitions.

Industrial applications of flutter for aircraft design have predominantly focused on studying classical flutter under idealized flow conditions from potential flow theory. Treatises on classical flutter have been widely established in a variety of foundational literature [2–4], and more modern treatments can be found in Refs. [5,6] with some nonlinear extensions [7]. This theory remains a reliable tool for engineers to efficiently design modern aircraft in subsonic and supersonic regimes, where flow disturbances are heavily simplified for analytical considerations. However, potential flow methods cannot reliably capture phenomena such as shock/boundary layer interactions (SBLIs) [8], multi-degree-of-freedom structures, vortex shedding, flow separation, and reattachment, especially at higher angles of attack [9]. These effects are especially prominent in transonic and more disturbed low supersonic regimes. As the industrial focus shifts toward designing energy-efficient [10] and lightweight aircraft with high-aspect-ratio configurations [11,12] in these flow regimes, it

[1]Corresponding author.

Contributed by the Applied Mechanics Division of ASME for publication in the Journal of Applied Mechanics. Manuscript received November 13, 2023; final manuscript received December 11, 2023; published online January 29, 2024. Assoc. Editor: Yashashree Kulkarni.

becomes imperative to adopt more precise flutter prediction methods based on high- and multi-fidelity methods.

Methods involving combinations of computational fluid dynamics and computational solid dynamics (CFD-CSD) have evolved to address these developments in aircraft design [13–15]. However, their high computational cost impedes widespread industrial adaptation [6,16]. Therefore, various approaches have been developed to incorporate varying CFD-CSD accuracy into flutter analysis, from corrective terms within analytical theories to real-time coupled fluid–structure interaction (FSI). The most comprehensive recent work summarizing these efforts was conducted by Xu et al. [17].

Alternatively, as unsteady CFD simulations are a primary driver of computational expenses in flutter analysis, research into reduced-order models (ROMs) has emerged as a prominent direction in flutter analysis. Various ROMs aim to capture the dominant contributing factors in the flutter model, thus achieving a significant simplification of the original high-fidelity model. The use of classical dimension-reduction methods or newly developed data-driven methods usually characterizes these ROMs.

The objective of this article is to provide a holistic overview of different methods developed for analyzing wing flutter in aircraft. The most common methods to analyze and predict flutter in aircraft systems are outlined in Fig. 1 and will be covered in Sec. 2: traditional and industrial potential theory-based approximations, research-oriented numerical finite simulations, and cost-effective hybrid ROM models. These methods have been developed to address very specific challenges of flutter phenomena at different flow regimes, as will be discussed in Sec. 3. Finally, in Sec. 4, a summary of recent optimization work with respect to standalone flutter optimization and flutter as part of a multidisciplinary design process will be provided.

Since aerodynamic theory frequently poses more significant limitations, particular emphasis is placed on elucidating flutter phenomena from an aerodynamic computational perspective and introducing previous research on flutter prediction. As there exists a vast amount of literature available on this topic, the current article aims to bring key highlights and recent developments together in one place.

2 Methods in Flutter Analysis

The following three sections aim to address how engineers and researchers compromise between flutter accuracy and computational speed for practical applications in aircraft design. In short, the traditional potential theory methods efficiently describe classical (harmonic) flutter within the majority of a flight envelope, while numerical (CFD-based) simulations capture more complex flow phenomena. The ROMs aim to reconcile the speed and accuracy of the aforementioned methods, providing a promising research direction for future multidisciplinary aircraft design and optimization (MDAO).

The three research methods involving potential flow theories, CFD simulations, and ROMs are closely related in their historical development and integration of shared techniques, as illustrated in Fig. 2, where three arrow types indicate the flow of information and data transfer between various analysis components. The left-hand side represents flow-related components, whereas the right-hand side follows structural elements. The outer loop follows traditional industrial flutter analysis methods based on more analytical formulations, shown in solid lines. Numerical and ROM-based approaches in dashed and double lines follow and expand upon this established flutter analysis procedure.

2.1 Analytical Potential Theory Methods. Traditional industrial methods, based on unsteady linearized potential flow equations, persist as a prevalent choice in the design and certification of modern aircraft [16]. Their primary advantage lies in their significantly lower numerical cost and the overall simplicity of models that incorporate the entire flow domain into boundary conditions, assuming linear, isentropic, inviscid, and irrotational flow conditions. The flow velocity $\mathbf{u}$ vector collapses to functions of potential ϕ and stream ψ equations, as follows:

$$\mathbf{u} = \nabla\phi \quad \text{for} \quad \nabla^2\phi = 0 \tag{1}$$

$$\mathbf{u} = \nabla \times \psi \quad \text{for} \quad \nabla^2\psi = 0 \tag{2}$$

Pressure estimations based on these assumptions constitute "panel codes" that model aerodynamic loads on surfaces divided into discrete elements.

The transformation of the fixed boundary from time domain to Laplace and Fourier configurations to eliminate flow dependence on coordinate variables constitutes the source of the most extensive numerical work using these codes [2]. Therefore, cost-effective stationary Cartesian meshes can be achieved [18]. Notable recent comparisons of potential flow methods in aircraft design and flutter

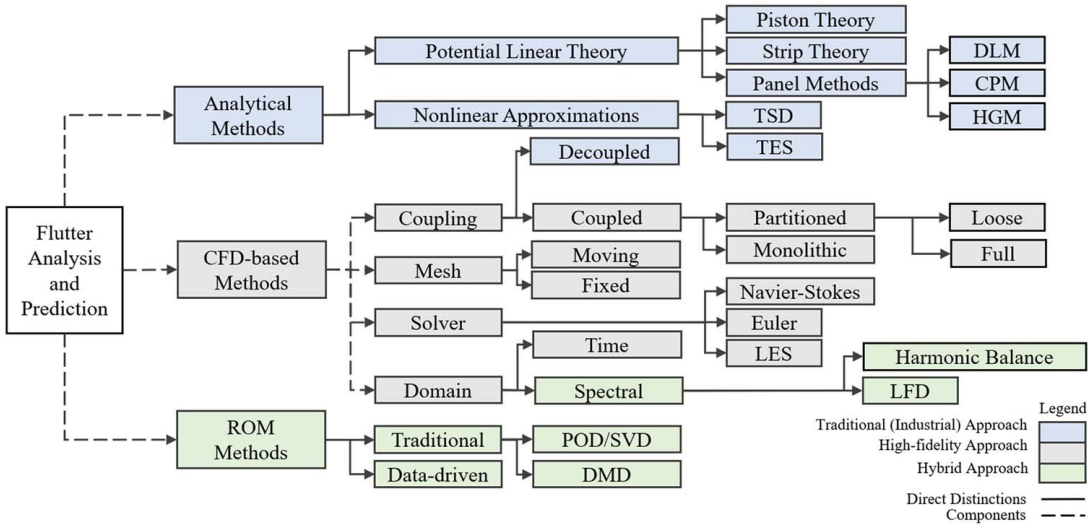

Fig. 1 Different technical frameworks for flutter analysis and prediction: analytical methods, CFD-based methods, and ROM-based methods. These methods can be further assessed from a performance perspective, with traditional approaches being highly efficient and high-fidelity methods being most accurate. Hybrid approaches harness traditional and novel data processing techniques to extract dominant behaviors from high-fidelity data.

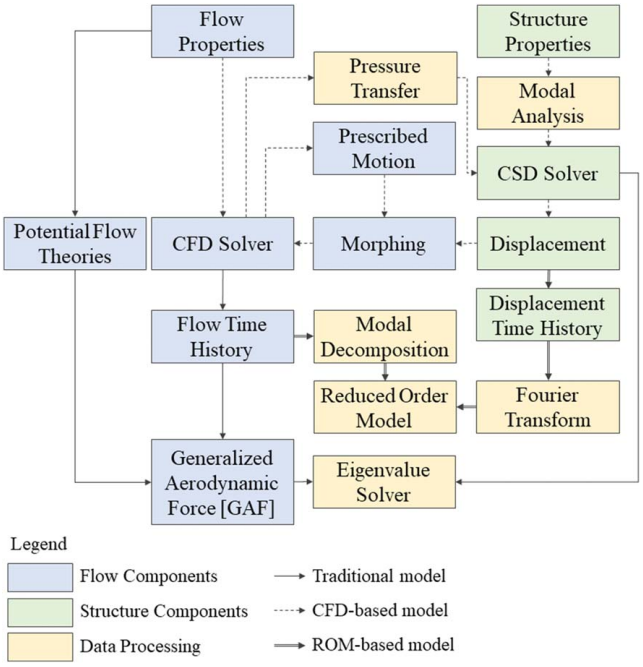

Fig. 2 Workflow depicting traditional, CFD-based, and ROM-based methods for flutter analysis. The outer layer follows the traditional model, combining decoupled flow and structure components. The inner-upper layer illustrates a fully CFD-based approach with continuously coupled components. The inner-lower layer depicts the ROM-based method, leveraging processing methods inspired by the traditional model together with high-fidelity CFD-based data.

analysis are offered by Kier et al. [12], emphasizing contemporary applications, and Wang and Li et al. [19], focusing on separated flows. The rest of this section outlines the overarching traditional industrial potential theory-based flutter analysis strategy and pertinent research extensions.

2.1.1 Formulation of the Aeroelastic Problem. Structural systems first undergo modal analysis to derive generalized coordinates. These coordinates feed into a structural solver, relating displacements, forces, and structural properties applicable to both rigid and continuous systems. A widely used tool for visualizing and probing aeroelastic principles is the rigid sectional model of an airfoil illustrated in Fig. 3(*a*). Its equations of motion are formulated via two generalized coordinates, twist α and vertical displacement h, which are given by Dowell [2]:

$$m\ddot{h} + K_h h + S_\alpha \ddot{\alpha} = -L, \quad \text{where } L \equiv \int p \, \mathrm{d}x \tag{3}$$

$$S_\alpha \ddot{h} + I_\alpha \ddot{\alpha} + K_\alpha \alpha = M_y, \quad \text{where } M_y \equiv \int px \, \mathrm{d}x \tag{4}$$

where m represents mass, S_α and I_α denote static moment and inertia around the rotation axis, respectively, while K_h and K_α stand for translational and torsional stiffnesses, respectively. The lift and bending moment are reflected via L and M, where p represents the pressure distribution derived from potential theory equations.

For continuous systems, like a cantilever beam, the finite element method can be used to create matrix-based equations, employing polynomials or preferably orthogonal shape modes as generalized coordinates, based on their availability. The more general form of Eqs. (3) and (4) then takes the following expression:

$$[M]\{\ddot{\eta}\} + [K]\{\eta\} = \{Q\} \tag{5}$$

where η is a generalized coordinate vector, M is a generalized mass matrix, K is a generalized stiffness matrix, and Q is a generalized aerodynamic force (GAF) vector.

2.1.2 Formulation of the Aerodynamic Loads. The generalized forces in the aeroelastic problem are formulated via pressure distributions obtained through the workflow on the left side of Fig. 2. The analytical derivations for these loads fall into time-integrated, harmonic, and indicial approaches, which are used to formulate readily interpretable panel codes [20]. These models can also be supplemented by wind tunnel and/or high-fidelity simulation data. The final GAF vector can be represented via a product of aerodynamic influence coefficient (AIC) matrices and generalized coordinates:

$$\{Q\} = [A]\{\eta\} + [B]\{\dot{\eta}\} + [C]\{\ddot{\eta}\} + [D]\{\lambda\} \tag{6}$$

where matrices A, B, C, and D represent AIC matrices and λ denotes "augmented" or "lag" states related to a flow field [5].

2.1.3 Formulation and Visualization of the Flutter Boundary. The AIC matrices allow the formulation of an eigenvalue problem, with the structural and aerodynamic components on the left-hand side of the generalized aeroelastic equation:

$$([M] - [C])\{\ddot{\eta}\} - [B]\{\dot{\eta}\} + ([K] - [A])\{\eta\} - [D]\{\lambda\} = \{0\} \tag{7}$$

Various eigenvalue finding techniques are available to accurately solve Eq. (7). The include the computationally extensive p method, the "classical flutter method" that neglects damping properties, the k or $U-g$ method that introduces artificial structural damping, and the widely used $p-k$ method acting as a compromise between the latter two [5].

The resolved real and imaginary eigenvalue components reflect the damping and frequency traits of structural modes, respectively. Iteration across the flow parameters reveals the aircraft's full flight envelope. Figure 3 outlines typical plots used to visualize the aeroelastic analysis: (*b*) time-marching plot of generalized amplitudes at fixed flow conditions, (*c*) eigenvalue magnitudes at increasing flow speeds, (*d*) transonic dip, and (*e*) and (*f*) limit cycle oscillation (LCO) amplitudes at an increased flow speed. The latter will be discussed in a later section.

Repeated stability analysis either in time (*b*) or spectral (*c*) form considering a variety of system parameters, such as temperature, pressure, and density, reveals a concise flight envelope graph often called the transonic dip (*d*). Typically, two side-by-side graphs are plotted as the Mach number increases: one detailing flight properties and the other flutter frequency ω_α. Flight properties are represented using either the velocity index ($U_f = \frac{U_\infty}{\omega_\alpha b_s \sqrt{\mu}}$) or dynamic pressure ($q = \frac{1}{2}\rho_\infty U_\infty^2$), with U_∞ and ρ_∞ signifying flow speed and density, and b_s being the root semi-chord. The mass ratio $\mu = \frac{\bar{m}}{\bar{V}\rho_\infty}$ involves wing mass $\bar{m}$ and conical frustum volume $\bar{V}$ of one wing. The flutter frequency is communicated either as is or via a frequency ratio against ω_α, the uncoupled first torsional natural frequency.

With respect to the latter set, a typical bifurcation diagram Figs. 3(*e*) and 3(*f*) is often used to visualize the nonlinear relationship between flutter amplitude and flow speed, particularly within the transonic regime. Two alternative branches communicate the stability of a chosen aeroelastic system. On the supercritical branch, flutter amplitude grows unbounded until nonlinearities stabilize it into a constant-amplitude LCO. On the subcritical branch, significant disturbances prior to the critical flutter speed may cause a break from equilibrium, suddenly jumping the amplitude of a system.

The traditional industrial potential theory-based flutter analysis and prediction procedure harnesses simple potential flow assumptions to resolve classical harmonic flutter for most flight conditions. The analytical equations for pressure distributions allow for readily interpretable and iterative analysis with respect to generalized

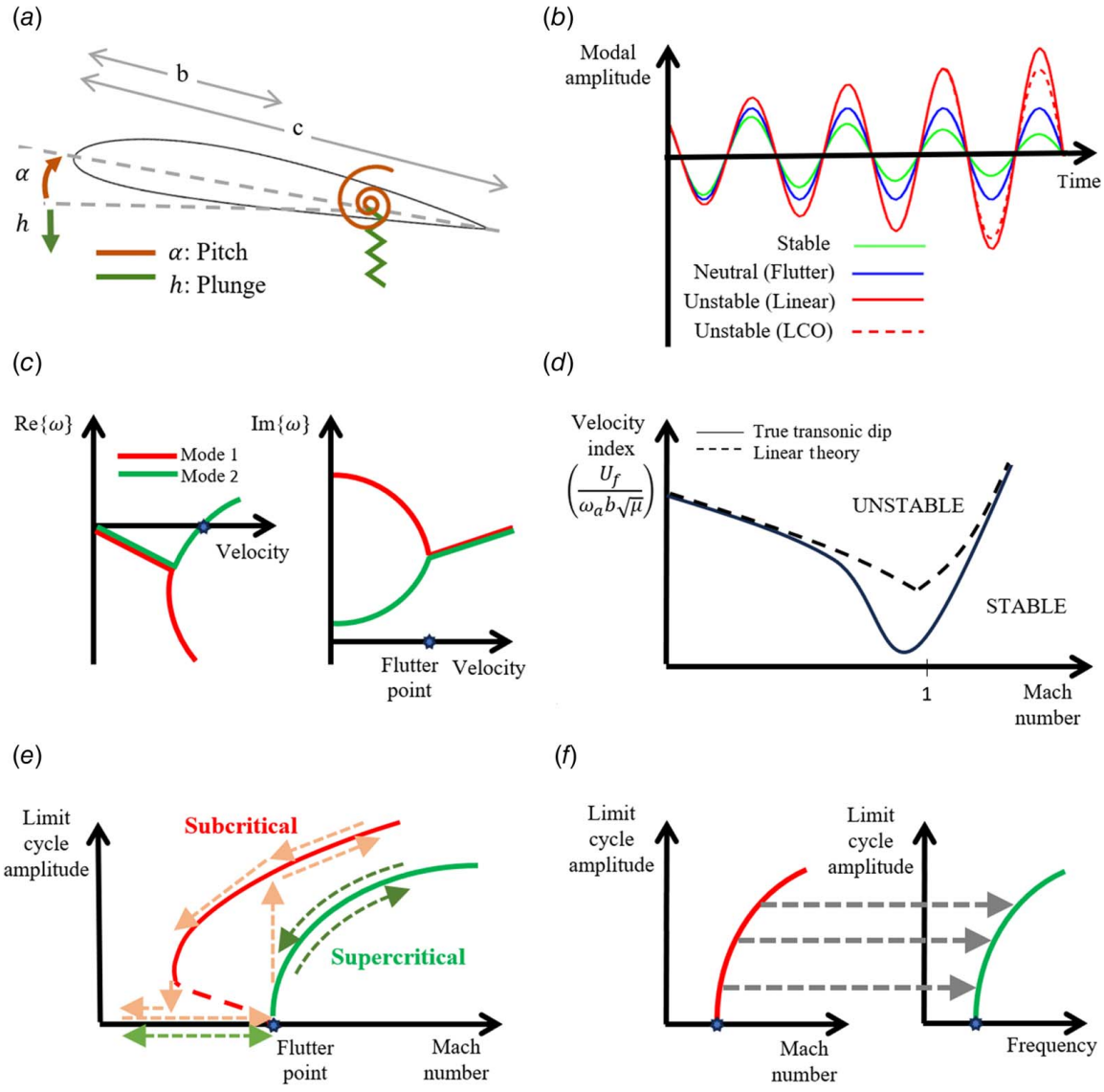

Fig. 3 (*a*) Wing section model: configuration of a two-dimensional pitch and plunge airfoil model, where *c* and *b* denote chord and half-chord, respectively. (*b*) Transient stability time history: pitching and plunging behavior of a converging stable system, neutral flutter, and diverging or plateauing in an LCO unstable system. (*c*) Flutter eigenvalue analysis: traditional eigenvalue stability analysis, predicting flutter when at least one mode's real component crosses the *x*-axis. (*d*) Flight envelope: configuration of the transonic dip in the transonic regime. (*e*) Postflutter stability bifurcation: comparison between subcritical and supercritical bifurcation diagrams for LCO. (*f*) Postflutter frequency bifurcation: bifurcation diagram relating Mach number and oscillation frequency for a given LCO amplitude.

equations of motion. These equations are solved via robust eigenvalue-solving techniques to produce various stability fronts within a flight envelope. This streamlined procedure remains popular for flutter prediction and analysis in most practical and multidisciplinary optimization applications.

2.2 Computational Fluid Dynamics-Based Methods. When local investigation into more complex phenomena is desired, methods based on computational fluid dynamics (CFD) become useful. These methods are predominantly split into coupled and decoupled approaches, which relate to the degree of data communication between flow and structure. Two excellent textbooks cover FSI fundamentals and applications: one by Bazilevs et al. [21], addressing general principles and a wide range of applications, and the other by Jaiman and Joshi [22], delving into up-to-date numerical FSI schemes and turbulence integration in depth. The following sections distinguish between decoupled and coupled schemes and highlight key developments used in CFD-based flutter analysis within industry and academic research.

2.2.1 Decoupled Methods. Decoupled techniques are generally used to correct or substitute GAF formulations in aeroelastic eigenvalue problems. This direct link to conventional flutter analysis procedures establishes these methods as a viable industrial choice for certifying and designing aircraft in more complex flow regimes [16]. Many popular decoupled approaches rely on spectral analysis to further enhance their computational efficiency.

The linearized frequency domain (LFD) method gained increased popularity following its integration into NASA's FUN3D in 2020 [23], alongside the incorporation of adjoint-based sensitivity capabilities [24]. This method decomposes the unsteady flutter response into a nonlinear mean and small linear perturbations around it. The decomposition is achieved by solving the flow response to

prescribed harmonic motions of structural modal shapes at various frequencies around a steady mean.

The methods based on classical harmonic balance (HB) procedure have also been gaining increased traction due to their superior applicability in shape optimization. The HB method was first adapted to CFD analysis by Hall et al. [25], who approximated unsteady flow via Fourier series with spatially varying coefficients of turbomachinery. As part of the method, flow is assumed to be steady periodic and aeroelastic variables are approximated as a truncated Fourier series as follows,

$$w(\mathbf{x}, t) = \hat{w}_0 + \sum_{n=1}^{N_H} [\hat{w}_{A,n}(\mathbf{x}) \cos(wnt) + \hat{w}_{B,n}(\mathbf{x}) \sin(wnt)] \quad (8)$$

The HB flutter analysis codes iterate directly on governing and structural equations, utilizing different combinations of prescribed mode shape amplitudes, frequencies, and flow parameters until a harmonic response is converged upon [26,27]. The efficiency of the algorithm was later improved upon to be independent of the number of structural degrees of freedom [28] and scalable using only one global solution vector [29]. Therefore, eigenvalue postprocessing steps are no longer necessary, making these methods viable for continuous optimization work.

2.2.2 Coupled Methods. Most modern coupled FSI schemes use a partitioned approach that iterates between flow and structural solvers to directly integrate separate software and to avoid overconstrained problems. Many papers also differentiate between loosely coupled and fully coupled solvers [9]. The main distinction lies in the frequency of data transfer across shared boundaries. Partitioned solvers, which perform many subiterations per time-step, as well monolithic solvers, which resolve the entire system simultaneously, are labeled as fully coupled schemes.

A standard procedure for conducting coupled aeroelastic time-marching analysis typically involves three main steps: (1) a steady simulation with rigid structure, (2) an unsteady simulation with static structure's damping set close to 1, and (3) a dynamic run from the converged deflection, optionally including a small gust excitation [30]. An alternative approach involves a prescribed oscillation instead of a static run, usually until steady flow is attained [31]. To ensure accurate results, sufficiently long test times are required to allow the initial transient to dissipate before the solution converges into a harmonic oscillation [9]. The flutter boundary can then be determined via iterative trials on system parameters to find a neutral harmonic transient. In more detail, McNamara and Friedmann [32] reviewed three time-domain system identification techniques to better extract damping, flutter boundary, and frequency data from the CFD-based general transient response.

2.2.3 Developments in Computational Fluid Dynamics. Most aeroelastic FSI research papers focus on development and implementation of more efficient and accurate flow and coupling solvers. These efforts can be split into three categories: turbulence modeling, underlying flutter physics, and parameter studies. The following section will highlight representative developments in each category.

Early attempts at coupled FSI often encountered challenges in accurately estimating supersonic conditions. Studies incorporating the full Reynolds-averaged Navier–Stokes (RANS) equations observed that viscous effects alone could not reduce the corresponding overestimation [33]. Consequently, efforts have been directed toward refining turbulence models for flutter prediction [34]. One notable achievement was the integration of detached-eddy simulation-based methods into flutter analysis. These approaches combine large eddy simulations (LES) for far-field regions with RANS for near-wall regions [35]. Further enhancements came through the incorporation of delayed detached eddy simulation methods [36] and improved wall modeling capability (IDDES) methods [37], both of which were originally formulated by Gritskevich et al. [38]. Notably, IDDES has demonstrated superior accuracy when compared to RANS coupled with various turbulence models in the context of flutter analysis, particularly in benchmark scenarios such as the AGARD 445.6 wing [39].

While RANS-LES simulations have the capability to capture complex transonic shock buffet, involving periodic shock and flow separation, investigations into RANS-only [40] or LFD-based [41] tools are still ongoing to reduce computational costs. Novel methods are also evolving to manage these costs without sacrificing accuracy, such as an "energy map" tool based on the amount of energy an airfoil extracts from the flow during various prescribed oscillations. This approach has been investigated for compressible [42] flows to predict flutter boundaries of two-dimensional airfoils.

The turbulence model developments are further used to investigate the underlying physics of various flutter phenomena. Using $k-\omega$ shear stress transport coupled with RANS, Ilie and Havenar [43] extensively visualized diverse effects of increasing Mach number and angle of attack on the strength, location, and interaction of shocks, flow separation, and wing deflection. The SBLI is another underlying cause of flutter actively studied over flexible structures [44].

Regarding specific flutter phenomena, Hammer et al. [45] further visualized how lower aspect wing ratios lead to a reduced onset in dynamic stall, which is related to wing oscillation past the static stall orientation. During closely related stall flutter, resulting from periodic flow separation, the suppression of LCOs can be achieved through momentum addition via slits [46].

The vast sensitivity of flow separation, shock, and viscous effects to flow and structure variables necessitates parameter uncertainty investigation for the future optimization work. These parameters span gas composition, Reynolds number, angle of attack [47], viscosity, and density [48]. The eventual goal is global sensitivity analysis, for example, shock locations in transonic flight [49].

2.2.4 Developments in Computational Solid Dynamics. Structural solvers are generally given less attention in FSI-related studies. Consequently, the work concerning CSD in FSI is scattered between analyzing (nonlinear) structures at a lower cost and conducting preliminary optimization studies. Once the nonlinear structural theory is validated using potential flow methods, unsteady RANS methods are employed to capture coupled nonlinear behaviors from both the structure and the flow around it, along with the corresponding LCOs associated with viscous effects [64]. As the solvers for both are often separate, with the appropriate load projection, the structural model does not necessarily need to match the geometry curves used for calculating pressure distributions, offering reduced cost, and retaining accuracy [65].

2.2.5 Developments in Coupling Tools. The primary challenge of FSI lies in the precise and cost-effective integration of flow and structural solvers, achieved through a resilient mesh network and efficient load transfer mechanisms. This technical complexity emerges from the necessity to capture distinct reference systems commonly employed for flow and structural displacements. In addition, ensuring the consistent alignment of kinematic, dynamic, and geometric boundary conditions further contributes to the challenge.

The frequent choice for aeroelastic coupling involves deforming structured or unstructured mesh around a moving body via arbitrary Lagrangian–Eulerian (ALE) and similar methods. Introducing relative grid movement into the compressible continuity and momentum N-S equations results in the following expressions, respectively:

$$\frac{\partial \rho^f}{\partial t} + \nabla \cdot \left(\rho^f \left[\mathbf{u^f} - \mathbf{u^m}\right]\right) = 0 \quad (9)$$

$$\frac{\partial}{\partial t}\left(\rho^f u_i^f\right) + \nabla \cdot \left(\rho^f u_i^f \left[\mathbf{u^f} - \mathbf{u^m}\right]\right) = -\frac{\partial p}{\partial x_i} + \nabla \cdot \left(\mu \nabla u_i^f\right) \quad (10)$$

where $\mathbf{u^f}$ and $\mathbf{u^m}$ represent the local flow and nodal velocity vectors, respectively, ρ^f and μ are flow density and viscosity, respectively, p denotes pressure, and the subscript i corresponds to a Cartesian

vector component [66]. Since mesh displacement solely affects the flow domain, the continuous structure formulation remains unchanged.

In partitioned approaches, mesh node motion is related to structural motion via an interpolation matrix, which can also relate fluid and structure tractions. Controlling mesh quality, particularly during large deflections, demands supplementary techniques beyond just defining initial properties, aimed at preventing negative volume cells and significant cell skewness [34]. Zhong and Xu further improved upon this traditional ALE coupling procedure, introducing a novel efficient modal approach for the deforming mesh that significantly reduced computational cost of AGARD 445.6 wing flutter analysis [67].

Despite readily available flow and structural solvers, achieving their robust coupling demands substantial numerical expertise. To streamline the coupling process for studies focused on flow or structural properties, there is a growing need for an automated, user-friendly, and open-source workflow [68].

The PRECICE library, a vast open-source parallel interpolation tool, is extensively employed in various coupled FSI software developments [69]. The capabilities of coupling with PRECICE were outlined by Chourdakis et al. in a discussion about FSI options within widely used open-source software, OPENFOAM [70]. Furthermore, specific solvers within OPENFOAM can be optimized for flutter analysis [71,72].

Among the numerous FSI frameworks constructed from the ground up, SU2 stands out as another popular choice for a cfd solver [73,74]. Notably, SU2 comes with built-in structural and interpolation solvers, showcasing its standalone robustness and efficacy for a wide range of FSI applications, including flutter analysis [75,76].

These integrated schemes allow for a growing integration of CFD into general flutter analysis, enabling the capture and increased understanding of complex flow phenomena beyond simple harmonic flutter. Coupled methods offer high-fidelity data at a high numerical cost, while decoupled methods compromise better between the two requirements. A similar conclusion is reached for time integrated versus spectral approaches. Harnessing the power of the latter, the reduced-order models build further upon them to reduce costs and maximize the accuracy of CFD-based flutter analysis models.

2.3 Reduced-Order Models. ROMs are developed to simplify the complex and computationally expensive high-fidelity systems. Similar to how spectral CFD-based methods reduce numerical cost, ROMs aim to capture the most dominant behaviors of a full-order system through a finite number of modes. Various ROM schemes can be split into traditional and data-driven self-learned categories based on the implemented analytical techniques.

2.3.1 Traditional Reduced-Order Models. Traditional ROMs take advantage of primarily projection-based methods. Higher-order dimensions are projected to several principal bases, thus reducing complexity. Lucia et al. [77] provided detailed documentation on traditional ROM development and classification. Some classic and popular methods will be highlighted here.

One of the most common projection-based methods in ROM is proper orthogonal decomposition (POD), also known as single value decomposition (SVD) [78]. POD is a powerful method in data analysis as it uses low-dimensional approximations to describe high-dimensional quantities (such as turbulent flow, vibrations). For an $N \times m$ data matrix A, where N and m can represent the temporal and spatial dimensions of the interested analysis, for example, the static pressure history of every element in a CFD analysis, one computes the singular value decomposition of A and derives

$$A = U\Sigma V^T \tag{11}$$

where U and V are orthogonal matrices and Σ gives the singular values σ_i of A. By applying the kth-order lower-rank approximation, the first k singular values are maintained, and all the other unselected singular values are set to zero. Now A can be approximated as follows:

$$A_k = U\Sigma_k V^T \tag{12}$$

and the first k columns of V are proper orthogonal modes. POD-based ROM models are often used to predict flutter for 2D airfoil or 3D wing [58,59,61]. They extract dominant modes from snapshot data and construct the ROM model to represent the full-order model. They have also been proven successful in nonlinear systems, as presented in some early literature [79,80]. Dynamic mode decomposition (DMD) is another dimension reduction method focusing more on temporal behaviors. It is, to some

Table 1 Recent ROM applications in multiple aeroelasticity studies

Reference	Background theories	Main application	Suitable flow regime	Validation	AI use
Cunha-Filho et al. [50]	Ritz basis	Aeroviscoelastic panel flutter analysis	Supersonic	Experiment	None
Brouwer et al. [51]	Piston theory	Shock/boundary layer interaction	Supersonic	Experiment	None
Nikbay et al. [52]	Polynomial chaos expansion; POD	Aeroelastic analysis on semi-span transport wing	Supersonic	Numerical simulation	None
Tian et al. [53]	Component mode synthesis technique	Nonlinear aeroservoelastic analysis	Supersonic	Numerical simulation	None
Akhavan et al. [54]	Piston theory; principle of virtual work	Stability and bifurcations analysis of laminate vibration	Supersonic	Numerical simulation	None
Berci et al. [55]	Modified strip theory; thin airfoil theory	Aeroelastic analysis of flexible wings with arbitrary planform	Subsonic	Numerical simulation	None
Gendelman et al. [56]	Complexification or averaging; slow-fast partition of the dynamics	Instability suppression rigid wings	Subsonic	Experiment; numerical simulation	None
Thomas et al. [57]; Hall et al. [58]; Lieu and Lesoinne [59]	POD	General wing configuration	Transonic	Numerical simulation	None
Zhou et al. [60]	POD	CFD-based flutter suppression with control delay	Transonic	Experiment; numerical simulation	None
Zhang and Ye [61]	POD	Flutter analysis of airfoil with control surfaces	Transonic	Numerical simulation	None
Liu et al. [62]	Discrete empirical interpolation method; Kriging technique	General 2D flutter boundary prediction	Transonic	Numerical simulation	Yes
Li et al. [63]	LSTM network	General 2D flutter boundary prediction	Transonic	Numerical simulation	Yes

Note: POD, proper orthogonal decomposition; LSTM, long short-term memory.

Table 2 Flow regimes defined by flutter applications

	Subsonic	Transonic	Supersonic	Hypersonic
Mach number [6]	$M<0.75$	$0.75<M<1.2$	$1.2<M<5$	$M>5$
Applications Flow quality	Propeller aircraft No shocks	Commercial turbofan aircraft Locally attached shocks; SBLI	Military turbojet aircraft Separated shocks with limited upstream disturbance propagation; SBLI	Rocket boosters Strong separated shocks with high-temperature induced flow effects; SBLI
Flutter	Classical flutter; stall flutter at high angles of attack [81]	Classical flutter; single DOF transonic buzz of a control surface; stall flutter; transonic buffet interaction [82];	Classical flutter; single DOF transonic buzz of a control surface; stall flutter	Classical flutter; stall flutter
Analytical solutions	Widely used: strip theory [83]; DLM [12]; VLM [12]	Sparsely used: TSD [10]	Widely used: Piston theory [84]; HGM [85]; CPM [86];	–
CFD-based solutions	Rarely used due to redundancy with analytical schemes; excellent match across most codes	Widely used: spectral domain, such as HB and LFD, is most efficient; time domain, such as RANS and LES, is most accurate	Moderately used (low-supersonic): increased influence of higher modes [87]; supplement analytical data [88]; complex shock behavior [89]	–
ROM solutions	Limited implementation based on analytical solutions [55,56,90]	Rising popularity: POD-based [58–61]; surrogate approach with LSTM [62]; physics-based low-order [91]	Moderate implementation based on hybrid of analytical solutions and CFD-based data [50,51]	

Note: DOF: degree-of-freedom; VLM: vortex lattice method; HGM; harmonic gradient method; and TSD: transonic small disturbance.

extent, more physically meaningful when dealing with flutter prediction problems. For a dynamic system

$$\frac{d\mathbf{x}}{dt} = f(\mathbf{x}, t, \mathbf{u}, \beta) \tag{13}$$

where $\mathbf{x}$ is the state vector, t is time, $\mathbf{u}$ is the actuation vector, and β represents all other parameters, given two sets of data $X^1 = [\mathbf{x}_1, \mathbf{x}_2, \ldots, \mathbf{x}_{m-1}]$, $X^2 = [\mathbf{x}_2, \mathbf{x}_3, \ldots, \mathbf{x}_m]$. The goal of DMD is to compute the eigenmodes and eigenvalues of A such that $X^2 \approx AX^1$ without calculating A itself. An SVD-based DMD process starts with the SVD of X^1: $X^1 = U\Sigma V^T$. Next, $\tilde{A}$ is calculated as follows:

$$\tilde{A} = U^T X^2 V \Sigma^{-1} \tag{14}$$

The eigenvalues σ of $\tilde{A}$ serve as the DMD eigenvalue. The DMD eigenmodes would be $U\mathbf{y}_i$, where $\mathbf{y}_i$ is the eigenvector of $\tilde{A}$. Unlike POD, the eigenmodes of DMD may not be orthogonal, but they are dynamically invariant. DMD has been applied to describe nonlinear flows by decomposing the flow into modes that share identical frequency and growth rate. The modes can be viewed as a nonlinear generalization of global eigenmodes of the linearized system [92].

2.3.2 Data-Driven Self-learned Reduced-Order Models. In recent years, there has been a surge of data-driven and artificial intelligence (AI)-based approaches to solve mechanics and materials problems [93–100]. Researchers have also sought self-learned models that describe the underlying relations between input and output in flutter analysis. The surrogate model predicts desired results, for example, CFD outputs, without or partially solving the full-order nonlinear system. Such data-driven approaches are mostly successful in CFD-based ROMs. For example, Zhang et al. [101] applied radial basis function neural network in a highly nonlinear aerodynamic ROM for limit cycle oscillation (LCO) analysis. Zhang et al. [102] also enhanced the generalization capability of nonlinear aerodynamic data-driven ROMs by introducing validation data.

As flutter analysis still relies on physical models, recent focus has been placed on formulation of hybrid ROMs that concurrently implement multiple background theories and data-driven techniques. This interest reflects rising specialization of aeroelasticity research, emphasizing particular case scenarios. Mallik et al. [103] presented one such scenario. They raised a fast transonic flutter prediction ROM by imposing an indicial function to unsteady CFD, adding a correction to strip theory and taking advantage of a steady CFD database. The resulting ROM-reduced finite wing analysis to an infinite airfoil case without taking any unsteady CFD simulation. Similar research examples are further presented in Table 1.

In general, the application of ROMs requires the statement of the corresponding flow regime. Since the transition from subsonic to hypersonic speed switches the flow from incompressible to compressible, the significant change in the fluid properties makes it challenging for the ROM to capture all of them. Therefore, current flutter analyses are mostly separated into various flow regimes.

3 Flutter Analysis for Various Flow Regimes

Different flutter analysis methods exhibit unique strengths and weaknesses at corresponding flow regimes: subsonic, transonic, and supersonic/hypersonic. In short, analytical methods are most

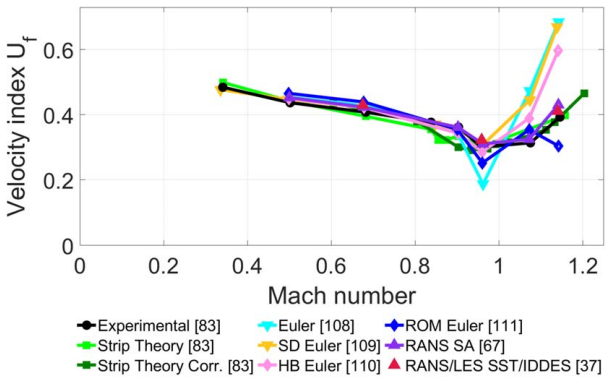

Fig. 4 Comparison of various flutter prediction models in relation to the transonic dip graph of weakened model #3 of AGARD 445.6 wing

Table 3 Selection of recent papers with flutter constraint within multidisciplinary aircraft design optimization

Reference	Tools	Flow	Methods	Subject	Objective	Flutter constraint	Variables
Boncoraglio and Farhat [115]	Euler; POD	Transonic	Nonlinear active manifold	CRM aircraft	Max lift to drag ratio	Lower bound on damping of all modes; bounded geometry;	Thicknesses of tail, wing, airfoil; wing shape
Abu-Zurayk et al. [116]	RANS; $p-k$ method	Flight envelope	Adjoint; Pareto fronts; OpenAD	XRF1 long-range wide-body aircraft	Min empty mass; min fuel burn	Negative damping of first 20 modes; structure strength, buckling; control surface efficiency	Shape of airfoil, wing, and fuselage; thicknesses of the wing box
Jacobson and Stanford [117]	LFD; DLM; $p-k$ method	Transonic; subsonic	Adjoint; OpenMDAO	Isogai wing; AGARD 445.6 wing	Min sum of FFD points; min mass	$KS_{flutter}<0$; target flight envelope	FFD airfoil shape points; wing shape
Khan et al. [118]	Indicial; steady RANS adjusted	Transonic	Particle swarm optimization	Truss-braced and cantilever wings	Max take-off gross mass; min fuel mass	Minimum flutter margin; bounded flight envelope, geometry, and performance; target C_L	Thrust; altitude; wing shape; strut locations
Sohst et al. [136]; do Vale et al. [137]	RANS: SST $k-\omega$; Nastran; $p-k$ method	Transonic	Kriging	HARW	Min structural mass; min fuel burn	Minimum flutter margin; maximum allowed yield stress	Factors of span, chord; thicknesses of the wing box; wing twists
Gray et al. [138]	RANS; strip theory	Subsonic	Adjoint	HARW	Cruise range	$KS_{flutter}<0$; $KS_{stress}<1$; target lift	Thicknesses of the wing box; span; sweep; angles
Xie et al. [139]	VLM; DLM; $p-k$ method	Subsonic	Direct search	HARW	Min mass	Bounded V_f; tip deflection, and stress; constant material	Beam section widths and thicknesses
Jonsson et al. [140]	DLM; $p-k$ method	Subsonic	Adjoint	Cantilever wing	Max range	$KS_{flutter}<0$; target C_L; bounded flight envelope; fixed plate area	Plate span, chord, and thickness
Ranjan and James [141]	DLM; classical HB	Subsonic	Gradient based; topology optimization	Cantilever NACA0012 wing	Max V_f; min C_D; min compliance	Binary flutter analysis; maximum V_f; constant C_L to C_D	Airfoil curvature parameters, density, centers of gravity and elastic axis
Shrivastava et al. [142]	DLM; Zona-51; $p-k$ method	Subsonic; supersonic	GA	Composite cantilever wing	Min mass	Maximum critical V_f; bounded geometry, wing twist, and tip deflection	Thicknesses and orientations of sub-laminates;
Kusni et al. [143]	MSC Nastran	Supersonic	Gradient based	Cantilever wing-box model	Min mass	Maximum damping of all modes; maximum tensile stress; constant material; bounded geometry	Thicknesses of the wing box
Faïsse et al. [144]	Quasi-static	Subsonic	Feedback loop; Pareto fronts	Cantilever beam	Min mass; max V_f	Maximum V_f; constant geometry and material	Thicknesses of a beam cross section
Riso et al. [133]	Quasi-static	Subsonic	Gradient based	Flat-plate section model	Min mass	$KS_{flutter}+KS_{postflutter}<0$	Mass ratio; stiffness coefficient
Li et al. [145]	Piston theory	Supersonic	Parametric	Functionally graded piezoelectric plate	Max V_f; min thermal buckling	Iterative flutter analysis; constant volume	Volume fractions; layer thicknesses; self-actuated active control

Note: SA, Spallart–Allmaras; SST, shear stress transport; HB, harmonic balance; GA, genetic algorithm; C_L, lift coefficient; HARW, high-aspect ratio wing; CRM, common research model; HH, Hicks–Henne; FFD, free-form deformation.

Table 4 Selection of recent papers focused on development of flutter-oriented optimization

Reference	Tools	Flow	Methods	Subject	Flutter objective	Other constraints	Variables
Jacobson et al. [119]	Euler	Flight envelope	Adjoint	AGARD 445.6 wing	Min dynamic pressure	KS damping function	Dynamic pressure
Palakurthy et al. [120]	RANS: SST	Supersonic	Parametric	Flexible panel	Max V_f; min LCO amplitude	Constant geometry and flow parameters	Dynamic pressure; micro-vortex generator presence
Prasad et al. [127]	Euler-based HB	Transonic	Adjoint	Isogai airfoil; AGARD 445.6 wing	Max V_f	Constant average structural energy and phase; target drag	HH airfoil shape functions
He et al. [128]	Euler-based HB	Transonic	Adjoint	Isogai airfoil; AGARD 445.6 wing	Max V_f	Bounded geometry; target average C_L	FFD airfoil and wing shape points
Thomas and Dowell [129]	RANS-based HB	Transonic	Adjoint	NLR 7301 and NACA 0012 airfoils	Max V_f	Target steady lift-to-drag ratio	Airfoil shape coordinates
Bilpriya et al. [125]	DLM; ZONA51; piston theory; $p-k$ method	Flutter envelope	Parametric	Rocket fin	Max flutter margin	Constant geometry	Mass distribution
Fazilati and Khalafi [121]	Piston theory	Supersonic	GA	Tow-steered composite panel	Max flutter dynamic pressure	Bounded fiber orientations; limited fiber curvature	Fiber direction; panel edges; layup traits
Tian et al. [122]	Piston theory	Supersonic	Parametric	Metamaterial plate embedded with resonators	Min modal amplitude	Constant damping coefficient and mass ratio	Dynamic pressure; frequency and number of local resonators
May et al. [126]	Piston theory	Supersonic	GA	Panel with inerters	Max flutter dynamic pressure	Bounded mass ratios and locations of inerters	Effective mass ratios; locations of inerters
Asadi et al. [123]	Indicial functions	Subsonic	Active/ passive; GA	Composite thin-walled beam wing–engine system	Min total aeroelastic energy	Bounded fiber angles, engine locations; constant flight speed	Fiber paths; piezo-composite actuators
Basta et al. [124]	Quasi-steady theory	Subsonic	Parametric	Metamaterial rigid airfoil attached to vibration absorbers	Max V_f; min LCO amplitude	Constant mass	Mass distribution and stiffnesses of vibration absorbers
Farrokh and Fallah [131]	Theodorsen's theory	Subsonic	Adaptive SVM; GA	Composite cantilever beam with an attached engine	Exact flutter boundary; max V_f	Bounded fiber angles	Flutter boundary; fiber angles
Garcia Pérez et al. [130]	Theodorsen's theory	N/A	Nonlinear energy sink; data-driven GA	Airfoil section with a flap	Max V_f; max/min total stability; min subcritical response	Constant geometry	Flap geometry and damping parameters; flow speed

Note: SA, Spallart–Allmaras; SST: shear stress transport; HB, harmonic balance; GA, genetic algorithm; SVM, support vector machine; C_L, lift coefficient; HARW, high-aspect ratio wing; CRM, common research model; HH, Hicks–Henne; FFD, free-form deformation.

successful at subsonic and supersonic conditions, while CFD-based methods excel at capturing transonic phenomena. Many ROMs spread thin across all regimes accelerating analysis either through robustly implementing analytical models or capturing only dominant modes of high-fidelity schemes. The summary of flow regimes defined by flutter applications are listed in the Table 2. Discussion of subsonic and supersonic regimes will not be continued further as industrial potential theory-based methods are well established there. With respect to the latter, Mei et al. [104] outlined classical developments in nonlinear panel flutter analysis at supersonic and hypersonic regimes, where more advanced treatment is concerned. In a similar manner, extensive discussion of transonic flutter is available given extensive difficulty to estimate it via analytical methods. The transonic regime is prone to high nonlinearity involving transonic dip [105] induced by compressibility effects as well as the oscillation of shock waves and their interaction with boundary layer and transonic buffet. Available analytical methods are limited to capture weak shocks and limited SBLI [106]. This situation compels engineers to incorporate larger safety margins into their estimations, resulting in less optimal designs and requiring extensive time to build corrective wind tunnel models [107]. Therefore, many CFD methods have been developed to capture complexities associated with the transonic regime, however, at an unpractical computational cost. Therefore, the development of ROMs has gained prominence due to the limitations of existing theories and the computationally expensive nature of numerical methods. For more detail, two studies are referred to for a complete treatment: Bendiksen [10], with an excellent overview of the unsteady transonic aerodynamics, and Gao and Zhang [82], with a more recent update.

Many aeroelastic schemes have been extensively tested on AGARD 445.6 weakened model 3, a 45 deg-sweptback thin airfoil wing tested at NASA's Transonic Dynamics Tunnel in 1987. Selected velocity index V_f results are compared to experimental transonic dip data in Fig. 4. Potential flow-based strip theory calculations, both before and after corrections with experimental data (circular markers), are indicated in square markers [83]. Euler-based results are portrayed from different perspectives, such as CFD-based in inverted triangle markers [108,109], harmonic balance [110] and ROM [111] in rhombus markers. High-fidelity studies based on complete Navier–Stokes equations are represented in triangle markers [37,67].

The general trends, analyzed and discussed by Silva et al. [108], suggest that the transonic dip's cause in AGARD 445.6 wing is likely compressibility rather than phase lag of the shock motion given the quality of prediction of strip theory in approximating the curve. The thin airfoil of the wing encourages these findings. Nevertheless, Stanford and Jacobson's recent discussion (2023) [112] on the AGARD model's transonic dip stresses importance of viscous effects, accurate tunnel boundary wall modeling, and broader data exploration as implied by general increase in accuracy of methods incorporating these effects into the evaluation.

4 Flutter Optimization

For a comprehensive review, Jonsson et al. extensively outlined history, background, and execution of flutter and postflutter optimization studies [113]. In the present review paper, Tables 3 and 4 list more recent developments in the flutter optimization field, particularly highlighting shape optimization efforts.

For the papers listed, two main research directions are observed for aircraft flutter optimization. Table 3 lists the recent studies that integrate flutter analysis into overall MDAO frameworks as part of the first direction. For more context, Martins and Kennedy outlined their experiences with large-scale multidisciplinary design optimization (MDO) through adjoint sensitivity analysis, categorizing various MDO methods and covering principles of structural sensitivity analysis [114].

In most MDO studies, the presence of unstable modes is commonly controlled through a binary damping or flutter margin check during the iterative parameter optimization process. Mainly, potential theory-based aerodynamic tools are employed, with a few extensions to high-fidelity simulations [115–118]. While LFD-based studies and RANS-corrected methods extract damping properties used for stability check directly from analysis, a variety of analysis procedures exist to estimate them from CFD data, as discussed by Jacobson et al. [119].

The second flutter optimization approach instead focuses on directly improving the standalone procedure through material design [120–126], shape optimization [127–130], and streamlining the process [119,131,130]. The objectives and constraints in this approach are tailored more closely to flutter analysis, incorporating various flutter-adjacent parameters such as damping values, LCO amplitudes, and time-integrated or steady-state coefficients of lift.

In both approaches to optimization, many eigenvalue-based flutter procedures employ the Kreisselmeier–Steinhauser (KS) aggregation function to accumulate damping values to assess the stability of all structural modes [132]. Furthermore, optimization of the full aircraft structure, instead of its separate components, remains computationally challenging, with only a few attempts listed [115,116].

When numerous such parameters or high-fidelity simulations are employed, gradient-based methods become lucrative because they allow for a lower number of iterations compared to genetic algorithms [133]. However, these methods are inclined to converge on a local minimum. Therefore, gradient-free approaches are expected to gain attention in the future, along with increased computational power and the development of efficient flutter analysis methods. Machine learning falls within this category, and recent research on recurrent neural network and long short-term memory network-based regression models [63] or data-based reduced models [134,135] is expected to accelerate this trend. Already, early studies incorporating machine learning within MDAO with flutter constraints offer promising results [115,131].

5 Discussion and Conclusion

In this review article, flutter analysis and prediction have been approached holistically. The article outlines the technical intricacies of three the most common methods, discusses approaches associated with different flow regimes, and presents updated progress in optimization.

The traditional potential theory-based methods approximate subsonic and supersonic regions more closely, but strong shock waves, high temperatures, and chemical reactions still interfere with accurate modeling of the latter. Despite their limitations, these methods remain prevalent in analyzing flutter for industrial use and prototyping novel proposals due to their efficiency. The high-fidelity time-marching methods cannot compete with this low numerical cost despite advances in computing power. As a result, the development of low-order LFD, HB-based, and ROM systems remains an active research direction.

In a similar vein, flutter optimization studies primarily rely on gradient-based frameworks due to their independence from design variables. To further reduce costs while maintaining sufficient accuracy, gradient-free frameworks, especially machine learning-based methods, are expected to continue gaining attention.

Flutter is actively being investigated from multiple directions to achieve more efficient and accurate predictions. The careful consideration of initial and boundary conditions further adds complexity to these investigations. Therefore, only through a combined effort involving growing computing power, experimental work, and novel designs, can the future lightweight and energy-efficient aircraft be designed to ensure both safety and stability.

Acknowledgment

We acknowledge support from CITRIS and the Banatao Institute, Mechanical Engineering Sciences Graduate Fellowship, Prytanean Foundation, and Air Force Office of Scientific Research (Fund Number: FA9550-22-1-0420).

Conflict of Interest

There are no conflicts of interest.

Data Availability Statement

No data, models, or code were generated or used for this paper.

References

[1] Bisplinghoff, R., Ashley, H., and Halfman, R., 1996, *Aeroelasticity*, Dover Publications, New York.

[2] Dowell, E. H., 2021, *A Modern Course in Aeroelasticity* (Solid Mechanics and Its Applications), 6th ed., Springer, Cham.

[3] Bisplinghoff, R. L., and Ashley, H., 1962, *Principles of Aeroelasticity*, Wiley, New York (Reprinted by Dover Publ. 1975).

[4] Fung, Y., 1993, *An Introduction to the Theory of Aeroelasticity* (Fundamentals of Flutter Analysis), Dover Publications Inc., Mineola, NY, p. 205.

[5] Hodges, D. H., and Pierce, G. A., 2011, *Introduction to Structural Dynamics and Aeroelasticity* (Cambridge Aerospace Series), 2nd ed., Cambridge University Press, Cambridge, UK.

[6] Wright, J. R., and Cooper, J. E., 2015, *Introduction to Aircraft Aeroelasticity and Loads*, 2nd ed. (Aerospace), John Wiley & Sons, Chichester UK.

[7] Dimitriadis, G., 2017, *Introduction to Nonlinear Aeroelasticity*, John Wiley & Sons, Chichester, West Sussex, UK.

[8] Eitner, M. A., Ahn, Y. -J., Musta, M. N., Sirohi, J., and Clemens, N., 2023, "Effect of Ramp-Induced Shock/Boundary Layer Interaction on the Vibration of a Compliant Panel at Mach 5," AIAA SCITECH 2023 Forum, National Harbor, MD & Online, Jan. 23–27, pp. 1–10.

[9] Chen, X., Zha, G.-C., and Yang, M.-T., 2007, "Numerical Simulation of 3-D Wing Flutter With Fully Coupled Fluid–Structural Interaction," Comput. Fluids, **36**(5), pp. 856–867.

[10] Bendiksen, O. O., 2011, "Review of Unsteady Transonic Aerodynamics: Theory and Applications," Prog. Aerosp. Sci., **47**(2), pp. 135–167.

[11] Banneheka Navaratna, P. D., Pontillo, A., Rezgui, D., Lowenberg, M. H., Neild, S. A., and Cooper, J. E., 2023, "Numerical Investigations of Subscale Flexible High Aspect Ratio Aircraft on a Dynamic Wind Tunnel Rig," AIAA SCITECH 2023 Forum, National Harbor, MD & Online, Jan. 23–27, pp. 1–20.

[12] Kier, T. M., 2023, "Comparing Different Potential Flow Methods for Unsteady Aerodynamic Modelling of a Flutter Demonstrator Aircraft," AIAA SCITECH 2023 Forum, National Harbor, MD & Online, Jan. 23–27, pp. 1–16.

[13] Bendiksen, O., and Kousen, K., 1987, "Transonic Flutter Analysis Using the Euler Equations," 28th Structures, Structural Dynamics and Materials Conference, Monterey, CA, Apr. 6–8, pp. 1–11.

[14] Alonso, J., and Jameson, A., 1994, "Fully-Implicit Time-Marching Aeroelastic Solutions," 32nd Aerospace Sciences Meeting and Exhibit, Reno, NV, Jan. 10–13, pp. 1–12.

[15] Liu, F., Cai, J., Zhu, Y., Tsai, H. M., and Wong, A. S. F., 2001, "Calculation of Wing Flutter by a Coupled Fluid-Structure Method," J. Aircr., **38**(2), pp. 334–342.

[16] Garrigues, E., 2018, "A Review of Industrial Aeroelasticity Practices at Dassault iation for Military Aircraft and Business Jets," Aerospace Lab, **14**, pp. 1–34.

[17] Xu, M., An, X., Kang, W., and Li, G., 2021, *Modern Computational Aeroelasticity*, De Gruyter, Berlin, Boston.

[18] Batina, J. T., 2005, "Advanced Small Perturbation Potential Flow Theory for Unsteady Aerodynamic and Aeroelastic Analyses," Langley Research Center, Hampton, VA.

[19] Wang, Y., and Li, J., 2023, "A Comparison of Separated Flow Models in the Aeroelasticity of Slender Wings," AIAA SCITECH 2023 Forum, National Harbor, MD & Online, Jan. 23–27, pp. 1–20.

[20] Ballhaus, W. F., and Goorjian, P. M., 1978, "Computation of Unsteady Transonic Flows by the Indicial Method," AIAA. J., **16**(2), pp. 117–124.

[21] Bazilevs, Y., Takizawa, K., and Tezduyar, T. E., 2013, *Computational Fluid-Structure Interaction: Methods and Applications*, John Wiley & Sons, Chichester, West Sussex, UK.

[22] Jaiman, R. K., and Joshi, V., 2022, *Computational Mechanics of Fluid-Structure Interaction*, Springer Nature, Singapore.

[23] Jacobson, K., Stanford, B., Wood, S., and Anderson, W. K., 2020, "Flutter Analysis With Stabilized Finite Elements Based on the Linearized Frequency-Domain Approach," AIAA Scitech 2020 Forum, Orlando, FL, Jan. 6–10, pp. 1–14.

[24] Jacobson, K., Stanford, B., Wood, S. L., and Anderson, W. K., 2021, "Adjoint-Based Sensitivities of Flutter Predictions Based on the Linearized Frequency-Domain Approach," AIAA Scitech 2021 Forum, Virtual Online, Jan. 11–15 and 19–21, pp. 1-14.

[25] Hall, K. C., Thomas, J. P., and Clark, W. S., 2002, "Computation of Unsteady Nonlinear Flows in Cascades Using a Harmonic Balance Technique," AIAA. J., **40**(5), pp. 879–886.

[26] Li, H., and Ekici, K., 2018, "A Novel Approach for Flutter Prediction of Pitch–Plunge Airfoils Using an Efficient One-Shot Method," J. Fluids Structur., **82**, pp. 651–671.

[27] Li, H., and Ekici, K., 2019, "Aeroelastic Modeling of a Three-Dimensional Wing Using the Harmonic-Balance-Based One-Shot Method," AIAA Scitech 2019 Forum, San Diego, CA, Jan. 7–11, pp. 1-25.

[28] Thomas, J., and Dowell, E., 2018, "A Fixed Point Iteration Approach for Harmonic Balance Based Aeroelastic Computations," 2018 AIAA/ASCE/AHS/ASC Structures, Structural Dynamics, and Materials Conference, Kissimmee, FL, Jan. 8–12, pp. 1–10.

[29] He, S., Jonsson, E., Mader, C. A., and Martins, J. R. R. A., 2021, "Coupled Newton–Krylov Time-Spectral Solver for Flutter and Limit Cycle Oscillation Prediction," AIAA. J., **59**(6), pp. 2214–2232.

[30] Chwalowski, P., Massey, S. J., Jacobson, K., Silva, W. A., and Stanford, B., 2022, "Progress on Transonic Flutter and Shock Buffet Computations in Support of the Third Aeroelastic Prediction Workshop," AIAA SCITECH 2022 Forum, San Diego, CA & Online, Jan. 3–7, pp. 1–13.

[31] Gnesin, V., Rządkowski, R., and Kolodyazhnaya, L., 2000, "A Coupled Fluid-Structure Analysis for 3D Flutter in Turbomachines," Proceedings of the ASME Turbo Expo 2000: Power for Land, Sea, and Air, Munich, Germany, May 8–11, pp. 1–8.

[32] McNamara, J. J., and Friedmann, P. P., 2007, "Flutter Boundary Identification for Time-Domain Computational Aeroelasticity," AIAA. J., **45**(7), pp. 1546–1555.

[33] Sadeghi, M., Yang, S., Liu, F., and Tsai, H., 2003, "Parallel Computation of Wing Flutter With a Coupled Navier-Stokes/CSD Method," 41st Aerospace Sciences Meeting and Exhibit, Reno, NV, Jan. 6–9, pp. 1–11.

[34] Jacobson, K., Stanford, B., Kiviaho, J. F., Ozoroski, T. A., Park, M. A., and Chwalowski, P., 2021, "Multiscale Mesh Adaptation for Transonic Aeroelastic Flutter Problems," AIAA AVIATION 2021 FORUM, Virtual Online, Aug. 2–6, pp. 1–19.

[35] Spalart, P. R., 2008, "Detached-Eddy Simulation," Ann. Rev. Fluid Mech., **41**(1), pp. 181–202. .

[36] Gan, J.-Y., Im, H.-S., Chen, X.-Y., Zha, G.-C., and Pasiliao, C. L., 2017, "Delayed Detached Eddy Simulation of Wing Flutter Boundary Using High Order Schemes," J. Fluids Struct., **71**, pp. 199–216.

[37] Patel, P., and Zha, G., 2021, "Improved Delayed Detached Eddy Simulation of AGARD Wing Flutter With Fully Coupled Fluid-Structure Interaction," AIAA Scitech 2021 Forum, Virtual Event, Jan. 11–15 & 19–21, pp. 1–16.

[38] Gritskevich, M. S., Garbaruk, A. V., Schütze, J., and Menter, F. R., 2012, "Development of DDES and IDDES Formulations for the K-ω Shear Stress Transport Model," Appl. Sci. Res., **88**(3), pp. 431–449.

[39] Šekutkovski, B., Kostić, I., Simonović, A., Cardiff, P., and Jazarević, V., 2016, "Three-Dimensional Fluid–Structure Interaction Simulation With a Hybrid RANS–LES Turbulence Model for Applications in Transonic Flow Domain," Aerosp. Sci. Technol., **49**, pp. 1–16.

[40] Giannelis, N. F., Thornber, B., and Vio, G. A., 2021, "Rigid Buffet Response of the Benchmark Supercritical Wing for the Third Aeroelastic Prediction Workshop," AIAA SCITECH 2022 Forum, San Diego, CA & Virtual, Jan. 3–7, pp. 1–15.

[41] Houtman, J., and Timme, S., 2021, "Towards Global Stability Analysis of Flexible Aircraft in Edge-of-the-Envelope Flow," AIAA Scitech 2021 Forum, Virtual Event, Jan. 11–15 & 19–21, pp. 1–16.

[42] Turner, J., Seo, J. H., and Mittal, R., 2023, "Analysis of the Flow Physics of Transonic Flutter Using Energy Maps," AIAA SCITECH 2023 Forum, National Harbor, MD, Jan. 23–27, pp. 1–10.

[43] Ilie, M., and Havenar, J., 2023, "Dynamic Aeroelastic Instabilities of Fixed-Wing Aircraft in Transonic and Supersonic Flows Using a Fully-Coupled Model," AIAA SCITECH 2023 Forum, National Harbor, MD, Jan. 23–27, pp. 1–10.

[44] Shinde, V. J., McNamara, J. J., and Gaitonde, D. V., 2021, "Shock Wave Turbulent Boundary Layer Interaction Over a Flexible Panel," AIAA Scitech 2021 Forum, Virtual Event, Jan. 11–15 & 19–21, pp. 1–19.

[45] Hammer, P. R., Garmann, D. J., and Visbal, M. R., 2021, "Effect of Aspect Ratio on Swept Wing Dynamic Stall," AIAA AVIATION 2021 FORUM, Virtual Event, Aug. 2–6, pp. 1–22.

[46] Fagley, C. P., Seidel, J., and McLaughlin, T. E., 2016, "Flow Field Analysis of Fully Coupled Computations of a Flexible Wing Undergoing Stall Flutter," 46th AIAA Fluid Dynamics Conference, Washington, DC, June 13–17, pp. 1–10.

[47] Navrátil, J., Jirásek, A., Lofthouse, A. J., and Satchell, M., 2019, "Effect of Flow Parameters Variation on Flutter Boundary of Benchmark Supercritical Wing," AIAA. J., **57**(2), pp. 772–781.

[48] Nilsson, S., Yao, H.-D., Karlsson, A., and Arvidson, S., 2022, "Effects of Viscosity and Density on the Aeroelasticity of the ONERA M6 Wing From Subsonic to Supersonic Speeds," AIAA AVIATION 2022 Forum, American Institute of Aeronautics and Astronautics.

[49] Robinson, B. M., Yuan, W., and Poirel, D., 2020, "Global Sensitivity Analysis of Shockwave Location During Transonic Flight," AIAA AVIATION 2020 FORUM, Virtual Event, June 15–19, pp. 1–19.

[50] Cunha-Filho, A., Briend, Y., de Lima, A., and Donadon, M., 2018, "An Efficient Iterative Model Reduction Method for Aeroviscoelastic Panel Flutter Analysis in the Supersonic Regime," Mech. Syst. Signal. Process., **104**, pp. 575–588.

[51] Brouwer, K. R., Perez, R. A., Beberniss, T. J., Spottswood, S. M., and Ehrhardt, D. A., 2022, "Evaluation of Reduced-Order Aeroelastic Simulations for Shock-Dominated Flows," J. Fluids Structur., **108**, p. 103429.

[52] Nikbay, M., and Acar, P., 2015, "Multidisciplinary Uncertainty Quantification in Aeroelastic Analyses of Semi-Span Supersonic Transport Wing," 16th AIAA/ISSMO Multidisciplinary Analysis and Optimization Conference, Dallas, TX, June 22–26, pp. 1–16.

[53] Tian, W., Gu, Y., Liu, H., Wang, X., Yang, Z., Li, Y., and Li, P., 2021, "Nonlinear Aeroservoelastic Analysis of a Supersonic Aircraft With Control Fin Free-Play by Component Mode Synthesis Technique," J. Sound. Vib., **493**, p. 115835.

[54] Akhavan, H., and Ribeiro, P., 2021, "Stability and Bifurcations in Oscillations of Composite Laminates wWith Curvilinear Fibres Under a Supersonic Airflow," Nonlinear Dyn., **103**(4), pp. 3037–3058.
[55] Berci, M., and Cavallaro, R., 2018, "A Hybrid Reduced-Order Model for the Aeroelastic Analysis of Flexible Subsonic Wings—A Parametric Assessment," Aerospace, **5**(3), p. 76.
[56] Gendelman, O. V., Vakakis, A. F., Bergman, L. A., and McFarland, D. M., 2010, "Asymptotic Analysis of Passive Nonlinear Suppression of Aeroelastic Instabilities of a Rigid Wing in Subsonic Flow," SIAM J. Appl. Math., **70**(5), pp. 1655–1677.
[57] Thomas, J., Hall, K., and Dowell, E., 2003, "A Harmonic Balance Approach for Modeling Nonlinear Aeroelastic Behavior of Wings in Transonic Viscous Flow," 44th AIAA/ASME/ASCE/AHS/ASC Structures, Structural Dynamics, and Materials Conference, Norfolk, VA, Apr. 7–10, pp. 1–6.
[58] Hall, K., Thomas, J., and Dowell, E., 1999, "Reduced-Order Modeling of Unsteady Small Disturbance Flows Using a Frequency Domain Proper Orthogonal Decomposition Technique," 37th Aerospace Sciences Meeting and Exhibit, Reno, NV, Jan. 11–14, pp. 1–11.
[59] Lieu, T., and Lesoinne, M., 2004, "Parameter Adaptation of Reduced Order Models for Three-Dimensional Flutter Analysis," 42nd AIAA Aerospace Sciences Meeting and Exhibit, Reno, NV, Jan. 5–8, pp. 1–9.
[60] Zhou, Q., Li, D.-F., Da Ronch, A., Chen, G., and Li, Y., 2016, "Computational Fluid Dynamics-based Transonic Flutter Suppression With Control Delay," J. Fluids Struct., **66**, pp. 183–206.
[61] Zhang, W., and Ye, K., 2010, "Effect of Control Surface on Airfoil Flutter in Transonic Flow," Acta Astronautica, **66**(7–8), pp. 999–1007.
[62] Liu, H., Gao, X., and Huang, R., 2020, "Efficient Reduced-Order Aerodynamic Modeling for Fast Prediction of Transonic Flutter Boundary," Int. J. Dyn. Control, **8**(4), pp. 1080–1088.
[63] Li, W., Gao, X., and Haojie, L., 2020, "Efficient Prediction of Transonic Flutter Boundaries for Varying Mach Number and Angle of Attack Via LSTM Network," Aerospace Sci. Technol., **110**, p. 106451.
[64] Ritter, M., Fehrs, M., and Mertens, C., 2023, "Aerodynamic and Static Coupling Simulations of the Pazy Wing With Transitional CFD for the Third Aeroelastic Prediction Workshop," AIAA SCITECH 2023 Forum, National Harbor, MD & Online, Jan. 23–27, pp. 1–22.
[65] Yuan, W., Sandhu, R., and Poirel, D., 2021, "Fully Coupled Aeroelastic Analyses of Wing Flutter Towards Application to Complex Aircraft Configurations," J. Aerosp. Eng., **34**(2), p. 04020117.
[66] Slone, A. K., Pericleous, K., Bailey, C., Cross, M., and Bennett, C., 2004, "A Finite Volume Unstructured Mesh Approach to Dynamic Fluid–Structure Interaction: An Assessment of the Challenge of Predicting the Onset of Flutter," Appl. Math. Model., **28**(2), pp. 211–239.
[67] Zhong, J., and Xu, Z., 2017, "A Modal Approach for Coupled Fluid Structure Computations of Wing Flutter," Proc. Inst. Mech. Eng. G J. Aerosp. Eng., **231**(1), pp. 72–81.
[68] Rumpfkeil, M. P., and Beran, P. S., 2022, "Aeroelastic Analysis and Optimization Using FUNtoFEM of an Efficient Supersonic Air Vehicle," AIAA SCITECH 2022 Forum, San Diego, CA & Virtual, Jan. 3–7, pp. 1–11.
[69] Cinquegrana, D., and Vitagliano, P. L., 2021, "Validation of a New Fluid–Structure Interaction Framework for Non-Linear Instabilities of 3D Aerodynamic Configurations," J. Fluids Struct., **103**, p. 103264.
[70] Chourdakis, G., Schneider, D., and Uekermann, B., 2023, "OpenFOAM-preCICE: Coupling OpenFOAM With External Solvers for Multi-Physics Simulations," OpenFOAM J., **3**, pp. 1–25.
[71] Kassem, H. I., Liu, X., and Banerjee, J. R., 2016, "Transonic Flutter Analysis Using a Fully Coupled Density Based Solver for Inviscid Flow," Adv. Eng. Softw., **95**, pp. 1–6.
[72] Fereidooni, A., Grewal, A. K., Seraj, S., and Grzeszczyk, M., 2018, "Computational Aeroelastic Analysis Using an Enhanced OpenFOAM-Based CFD-CSD Solver," 2018 AIAA/ASCE/AHS/ASC Structures, Structural Dynamics, and Materials Conference, Kissimmee, FL, Jan. 8–12, pp. 1–19.
[73] Thomas, D., Cerquaglia, M. L., Boman, R., Economon, T. D., Alonso, J. J., Dimitriadis, G., and Terrapon, V. E., 2019, "CUPyDO—An Integrated Python Environment for Coupled Fluid-Structure Simulations," Adv. Eng. Softw., **128**, pp. 69–85.
[74] Zanella, A., Abergo, L., Caccia, F., Morelli, M., and Guardone, A., 2023, "Towards an Open-Source Framework for Fluid–Structure Interaction Using SU2, MBDyn and PreCICE," J. Comput. Appl. Math., **429**, p. 115211.
[75] Sanchez, R., Kline, H. L., Thomas, D., Variyar, A., Righi, M., Economon, T. D., Alonso, J. J., Palacios, R., Dimitriadis, G., and Terrapon, V., 2016, "Assessment of the Fluid-Structure Interaction Capabilities for Aeronautical Applications of the Open-Source Solver Su2," ECCOMAS Congress 2016, Crete Island, Greece, June 5–10, pp. 1498–1529.
[76] Simiriotis, N., and Palacios, R., 2022, "A Flutter Prediction Framework in the Open-Source SU2 Suite," AIAA SCITECH 2022 Forum, American Institute of Aeronautics and Astronautics.
[77] Lucia, D. J., Beran, P. S., and Silva, W. A., 2004, "Reduced-Order Modeling: New Approaches for Computational Physics," Prog. Aerosp. Sci., **40**(1–2), pp. 51–117.
[78] Chatterjee, A., 2000, "An Introduction to the Proper Orthogonal Decomposition," Curr. Sci., **78**(7), pp. 808–817.
[79] Beran, P. S., Lucia, D. J., and Pettit, C. L., 2004, "Reduced-Order Modelling of Limit-Cycle Oscillation for Aeroelastic Systems," J. Fluids Struct., **19**(5), pp. 575–590.
[80] Lucia, D. J., Beran, P. S., and King, P. I., 2003, "Reduced-Order Modeling of an Elastic Panel in Transonic Flow," J. Aircraft, **40**(2), pp. 338–347.
[81] Dimitriadis, G., and Li, J., 2009, "Bifurcation Behavior of Airfoil Undergoing Stall Flutter Oscillations in Low-Speed Wind Tunnel," AIAA. J., **47**(11), pp. 2577–2596.
[82] Gao, C., and Zhang, W., 2020, "Transonic Aeroelasticity: A New Perspective From the Fluid Mode," Prog. Aerosp. Sci., **113**, p. 100596.
[83] Yates, Jr. C. E., 1987, AGARD Standard Aeroelastic Configurations for Dynamic Response. Candidate Configuration I.-Wing 445.6, NASA Langley Research Center, Hampton, VA, Tech. Rep. NASA-TM-100492; Nas 1.15:100492.
[84] Zhang, W.-W., Ye, Z.-Y., Zhang, C.-A., and Liu, F., 2009, "Supersonic Flutter Analysis Based on a Local Piston Theory," AIAA. J., **47**(10), pp. 2321–2328.
[85] Liu, D. D., James, D. K., Chen, P. C., and Pototzky, A. S., 1991, "Further Studies of Harmonic Gradient Method for Supersonic Aeroelastic Applications," J. Aircr., **28**(9), pp. 598–605.
[86] Appa, K., 1987, "Constant Pressure Panel Method for Supersonic Unsteady Airload Analysis," J. Aircr., **24**(10), pp. 696–702.
[87] Wang, G., Zhou, H., and Mian, H. H., 2021, "Numerical Analysis on Modal Stability Characteristics of 2D Panel Flutter at Low Supersonic Speeds," J. Fluids Struct., **103**, p. 103296.
[88] Marzocca, P., Librescu, L., Kim, D.-H., and Lee, I., 2005, "Supersonic Flutter and LCO of Airfoils Via CFD/Analytical Combined Approach," 46th AIAA/ASME/ASCE/AHS/ASC Structures, Structural Dynamics & Materials Conference, Austin, TX, Apr. 18–21, pp. 1–10.
[89] Zhou, H., Wang, G., and Liu, Z., 2020, "Numerical Analysis on Flutter of Busemann-Type Supersonic Biplane Airfoil," J. Fluids Struct., **92**, p. 102788.
[90] Prasad, C. S., Kolman, R., and Pešek, L., 2022, "Meshfree Reduced Order Model for Turbomachinery Blade Flutter Analysis," Int. J. Mech. Sci., **222**, p. 107222.
[91] Opgenoord, M., Drela, M., and Willcox, K., 2019, "Influence of Transonic Flutter on the Conceptual Design of Next-Generation Transport Aircraft," AIAA. J., **57**(5), pp. 1973–1987.
[92] Rowley, C. W., Mezić, I., Bagheri, S., Schlatter, P., and Henningson, D. S., 2009, "Spectral Analysis of Nonlinear Flows," J. Fluid. Mech., **641**, pp. 115–127.
[93] Jin, Z., Zhang, Z., Demir, K., and Gu, G. X., 2020, "Machine Learning for Advanced Additive Manufacturing," Matter, **3**(5), pp. 1541–1556.
[94] Brunton, S. L., Noack, B. R., and Koumoutsakos, P., 2020, "Machine Learning for Fluid Mechanics," Annu. Rev. Fluid. Mech., **52**(1), pp. 477–508.
[95] Chen, C.-T., and Gu, G. X., 2023, "Physics-Informed Deep-Learning for Elasticity: Forward, Inverse, and Mixed Problems," Adv. Sci., **10**(18), p. 2300439.
[96] Lee, S., Zhang, Z., and Gu, G. X., 2022, "Generative Machine Learning Algorithm for Lattice Structures With Superior Mechanical Properties," Mater. Horiz., **9**(3), pp. 952–960.
[97] Moosavi, S. M., Jablonka, K. M., and Smit, B., 2020, "The Role of Machine Learning in the Understanding and Design of Materials," J. Am. Chem. Soc., **142**(48), pp. 20273–20287.
[98] Jung, J., Kim, Y., Park, J., and Ryu, S., 2022, "Transfer Learning for Enhancing the Homogenization-Theory-Based Prediction of Elasto-Plastic Response of Particle/Short Fiber-Reinforced Composites," Composite Struct., **285**, p. 115210.
[99] Yu, C.-H., Wu, C.-Y., and Buehler, M. J., 2022, "Deep Learning Based Design of Porous Graphene for Enhanced Mechanical Resilience," Comput. Mater. Sci., **206**, p. 111270.
[100] Lee, S., Zhang, Z., and Gu, G. X., 2023, "Deep Learning Accelerated Design of Mechanically Efficient Architected Materials," ACS. Appl. Mater. Interfaces., **15**(18), pp. 22543–22552.
[101] Zhang, W., Wang, B., Ye, Z., and Quan, J., 2012, "Efficient Method for Limit Cycle Flutter Analysis Based on Nonlinear Aerodynamic Reduced-Order Models," AIAA. J., **50**(5), pp. 1019–1028.
[102] Kou, J., and Zhang, W., 2016, "An Approach to Enhance the Generalization Capability of Nonlinear Aerodynamic Reduced-Order Models," Aerospace Sci. Technol., **49**, pp. 197–208.
[103] Mallik, W., Schetz, J. A., and Kapania, R. K., 2018, "Rapid Transonic Flutter Analysis for Aircraft Conceptual Design Applications," AIAA. J., **56**(6), pp. 2389–2402.
[104] Mei, C., Abdel-Motagaly, K., and Chen, R., 1999, "Review of Nonlinear Panel Flutter at Supersonic and Hypersonic Speeds," ASME Appl. Mech. Rev., **52**(10), pp. 321–332.
[105] Ashley, H., 1980, "Role of Shocks in the 'Sub-Transonic' Flutter Phenomenon," J. Aircr., **17**(3), pp. 187–197.
[106] Zhang, Z., Liu, F., and Schuster, D., 2006, "An Efficient Euler Method on Non-Moving Cartesian Grids With Boundary-Layer Correction for Wing Flutter Simulations," 44th AIAA Aerospace Sciences Meeting and Exhibit, Reno, NV, Jan. 9–12, pp. 1–18.
[107] Yurkovich, R., Liu, D., and Chen, P., 2001, "State-of-the-Art of Unsteady Aerodynamics for High Performance Aircraft," 39th Aerospace Sciences Meeting and Exhibit, Reno, NV, Jan. 8–11, pp. 1–15.
[108] Silva, W. A., Chwalowski, P., and Perry, B., 2014, "Evaluation of Linear, Inviscid, Viscous, and Reduced-Order Modelling Aeroelastic Solutions of the AGARD 445.6 Wing Using Root Locus Analysis," Int. J. Comut. Fluid Dyn., **28**(3–4), pp. 122–139.
[109] Pan, J., and Liu, F., 2019, "Wing Flutter Prediction by a Small-Disturbance Euler Method on Body-Fitted Curvilinear Grids," AIAA. J., **57**(11), pp. 4873–4884.
[110] Thomas, J., and Dowell, E. H., 2023, "Using Broyden's Method to Improve the Computational Performance of a Harmonic Balance Aeroelastic Solution

Technique," AIAA SCITECH 2023 Forum, National Harbor, MD & Online, Jan. 23–27, pp. 1–16.
[111] Lowe, B. M., and Zingg, D. W., 2022, "Flutter Prediction Using Reduced-Order Modeling With Error Estimation," AIAA. J., **60**(7), pp. 4240–4255.
[112] Stanford, B., and Jacobson, K., 2023, "Transonic Flutter Dips of the AGARD 445.6 Wing," AIAA SCITECH 2023 Forum, National Harbor, MD & Online, Jan. 23–27, pp. 1–13.
[113] Jonsson, E., Riso, C., Lupp, C. A., Cesnik, C. E. S., Martins, J. R. R. A., and Epureanu, B. I., 2019, "Flutter and Post-Flutter Constraints in Aircraft Design Optimization," Prog. Aerosp. Sci., **109**, p. 100537.
[114] Martins, J. R. R. A., and Kennedy, G. J., 2021, "Enabling Large-Scale Multidisciplinary Design Optimization Through Adjoint Sensitivity Analysis," Struct. Multidiscip. Optim., **64**(5), pp. 2959–2974.
[115] Boncoraglio, G., and Farhat, C., 2021, "Active Manifold and Model Reduction for Multidisciplinary Analysis and Optimization," AIAA Scitech 2021 Forum, Virtual Event, Jan. 11–15 & 19–21, pp. 1–20.
[116] Abu-Zurayk, M., Merle, A., Ilic, C., Goertz, S., Schulze, M., Klimmek, T., Kaiser, C., Quero Martin, D., Häßy, J., Becker, R.-G., Fröhler, B., and Hartmann, J., 2021, "Sensitivity-Based Generation of Pareto Fronts for Design of Powered Aircraft Subject to a Comprehensive Set of Loads," AIAA AVIATION 2021 FORUM, Virtual Event, Aug. 2–6, pp. 1–14.
[117] Jacobson, K., and Stanford, B., 2022, "Flutter-Constrained Optimization With the Linearized Frequency-Domain Approach," AIAA SCITECH 2022 Forum, San Diego, CA & Virtual, Jan. 3–7, pp. 1–17.
[118] Khan, K. H., Mallik, W., Kapania, R. K., and Schetz, J. A., 2021, "Distributed Design Optimization of Large Aspect Ratio Wing Aircraft With Rapid Transonic Flutter Analysis in Linux," AIAA Scitech 2021 Forum, Virtual Event, Jan. 11–15 & 19–21, pp. 1–16.
[119] Jacobson, K. E., Kiviaho, J. F., Kennedy, G. J., and Smith, M. J., 2019, "Evaluation of Time-Domain Damping Identification Methods for Flutter-Constrained Optimization," J. Fluids Struct., **87**, pp. 174–188.
[120] Palakurthy, S., Zope, A., Yan, Y., Collins, E. M., and Bhushan, S., 2022, "Analysis of Passive Panel Flutter Control Using Micro-Ramp," AIAA SCITECH 2022 Forum, San Diego, CA & Virtual, Jan. 3–7, pp. 1–24.
[121] Fazilati, J., and Khalafi, V., 2019, "Aeroelastic Panel Flutter Optimization of Tow-Steered Variable Stiffness Composite Laminated Plates Using Isogeometric Analysis," J. Reinf. Plast. Compos., **38**(19–20), pp. 885–895.
[122] Tian, W., Zhao, T., Gu, Y., and Yang, Z., 2021, "Supersonic Flutter Control and Optimization of Metamaterial Plate," Chin. J. Aeronaut., **34**(11), pp. 15–20.
[123] Asadi, D., Farsadi, T., and Kayran, A., 2021, "Flutter Optimization of a Wing–Engine System With Passive and Active Control Approaches," AIAA. J., **59**(4), pp. 1422–1440.
[124] Basta, E., Ghommem, M., and Emam, S., 2021, "Flutter Control and Mitigation of Limit Cycle Oscillations in Aircraft Wings Using Distributed Vibration Absorbers," Nonlinear Dyn., **106**(3), pp. 1975–2003.
[125] Bilpriya, Rajendran, S., Gandhi, P.A., and George, M., 2021, "Prevention of Flutter Instability in Control Surface of a Test Vehicle Through Parametric Studies," Proceedings of SECON 2020, Lecture Notes in Civil Engineering, Vol. 97, Springer, Cham.
[126] May, P., Li, H., and Yang, H. T., 2023, "Inerter-Based Eigenvector Orientation Approach for Passive Control of Supersonic Panel Flutter," Sci. China Ser. A Math., **11**(6), p. 1462.
[127] Prasad, R., Choi, S., and Patil, M., 2022, "Aerodynamic Shape Optimization Using a Time Spectral Coupled Adjoint for Nonlinear Aeroelastic Problems," Aerosp. Sci. Technol., **126**, p. 107495.
[128] He, S., Jonsson, E., and Martins, J. R., 2022, "Wing Aerodynamic Shape Optimization With Time Spectral Limit-Cycle Oscillation Adjoint," AIAA AVIATION 2022 Forum, Chicago, IL & Virtual, June 27–July 1, pp. 1–23.
[129] Thomas, J., and Dowell, E. H., 2020, "Discrete Adjoint Constrained Design Optimization Approach for Unsteady Transonic Aeroelasticity and Buffet," AIAA AVIATION 2020 FORUM, Virtual Event, June 15–19, pp. 1–13.
[130] García Pérez, J., Ghadami, A., Sanches, L., Michon, G., and Epureanu, B. I., 2022, "Data-Driven Optimization for Flutter Suppression by Using an Aeroelastic Nonlinear Energy Sink," J. Fluids Struct., **114**, p. 103715.
[131] Farrokh, M., and Fallah, M. R., 2023, "Flutter Instability Boundary Determination of Composite Wings Using Adaptive Support Vector Machines and Optimization," J. Brazil. Soc. Mech. Sci. Eng., **45**(3), p. 181.
[132] Kennedy, G. J., and Hicken, J. E., 2015, "Improved Constraint-Aggregation Methods," Comput. Methods Appl. Mech. Eng., **289**, pp. 332–354.
[133] Riso, C., Cesnik, C. E. S., Epureanu, B. I., and Teufel, P., 2021, "A Post-Flutter Response Constraint for Gradient-Based Aircraft Design Optimization," AIAA AVIATION 2021 FORUM, Virtual Event, Aug. 2–6, pp. 1–23.
[134] Fonzi, N., Brunton, S. L., and Fasel, U., 2023, "Data-Driven Modeling for Transonic Aeroelastic Analysis," J. Aircraft, pp. 1–13.
[135] Simiriotis, N., and Palacios, R., 2023, "A Numerical Investigation on Direct and Data-Driven Flutter Prediction Methods," J. Fluids Struct., **117**, p. 103835.
[136] Sohst, M., Afonso, F., and Suleman, A., 2022, "Optimization and Comparison of Strut-Braced and High Aspect Ratio Wing Aircraft Configurations Including Flutter Analysis With Geometric Non-Linearities," Aerospace Sci. Technol., **124**, p. 107531.
[137] do Vale, J. L., Sohst, M., Crawford, C., Suleman, A., Potter, G., and Banerjee, S., 2023, "On the Multi-Fidelity Approach in Surrogate-Based Multidisciplinary Design Optimisation of High-Aspect-Ratio Wing Aircraft," Aeronautical J., **127**(1307), pp. 2–23.
[138] Gray, A. C., Riso, C., Jonsson, E., Martins, J. R., and Cesnik, C. E., 2023, "High-Fidelity Aerostructural Optimization With a Geometrically Nonlinear Flutter Constraint," AIAA. J., **61**(6), pp. 2430–2443.
[139] Xie, C., Meng, Y., Wang, F., and Wan, Z., 2017, "Aeroelastic Optimization Design for High-Aspect-Ratio Wings With Large Deformation," Shock Vibration, **2017**, p. 2564314.
[140] Jonsson, E., Mader, C. A., Kennedy, G., and Martins, J. R., 2019, "Computational Modeling of Flutter Constraint for High-Fidelity Aerostructural Optimization," AIAA Scitech 2019 Forum, San Diego, CA, Jan. 7–11, pp. 1–27.
[141] Ranjan, P., and James, K. A., 2019, "Flutter Control Using Shape and Topology Optimization," AIAA Aviation 2019 Forum, Dallas, TX, June 17–21, pp. 1–11.
[142] Shrivastava, S., Tilala, H., Mohite, P. M., and Limaye, M. D., 2020, "Weight Optimization of a Composite Wing-Panel With Flutter Stability Constraints by Ply-Drop," Struct. Multidiscip. Optim., **62**(4), pp. 2181–2195.
[143] Kusni, M., Widiramdhani, M., and Hadi, B. K., 2021, "Sensitivity Study and Structural Optimization of an Aircraft Wing in the Maximum-Stress and Flutter Constraints," IOP Conf. Ser.: Mater. Sci. Eng., **1173**(1), p. 012058.
[144] Faïsse, E., Vernay, R., Vetrano, F., Alazard, D., and Morlier, J., 2021, "Adding Control in Multidisciplinary Design Optimization of a Wing for Active Flutter Suppression," AIAA Scitech 2021 Forum, Virtual Event, Jan. 11–15 & 19–21, pp. 1–13.
[145] Li, P., Yang, Z., and Tian, W., 2023, "Nonlinear Aeroelastic Analysis and Active Flutter Control of Functionally Graded Piezoelectric Material Plate," Thin-Walled Struct., **183**, p. 110323.